

COLLISIONAL RELAXATION OF A STRONGLY MAGNETIZED PURE
ELECTRON PLASMA (THEORY AND EXPERIMENT)*

T. M. O'Neil, P. G. Hjorth,[†] B. Beck, J. Fajans[‡] and J. H. Malmberg

Physics Department, Univ. of Calif. at San Diego, La Jolla, CA 92093 USA

1. INTRODUCTION

We say that an electron plasma is strongly magnetized when the cyclotron period is short compared to the duration of a close collision. The gyroangles for the electrons may then be thought of as a collection of high frequency oscillators and the remaining variables (the guiding center variables) as slowly varying parameters that modulate the high frequency oscillators. Loosely speaking, one expects the high frequency oscillators to resonantly exchange quanta (or action) with each other, but not with the slowly varying variables. More precisely, one expects the total action associated with the cyclotron motion (i.e., $\sum_j m v_{\perp j}^2 / 2\Omega$) to be an adiabatic invariant.^{1,2} Here, $\Omega = eB/mc$ is the cyclotron frequency and $v_{\perp j}$ is the component of the j^{th} electron velocity that is perpendicular to the magnetic field. For the simple case of a uniform magnetic field, one may equivalently say that the total perpendicular kinetic energy is an adiabatic invariant, and this paper discusses the influence of the invariant on the collisional relaxation of the electron velocity distribution.

On a short time scale, the adiabatic invariant is well conserved, and there is negligible exchange of energy between the parallel and the perpendicular degrees of freedom. The distribution of parallel velocities and the distribution of perpendicular velocities relax separately to Maxwellian, with the parallel temperature (T_{\parallel}) not necessarily equal to the perpendicular temperature (T_{\perp}). However, the evolution does not stop at this stage, since an adiabatic invariant is not strictly conserved; it suffers exponentially small changes. In the present case, each collision produces an exponentially small exchange of energy between the parallel and the perpendicular degrees of freedom, and these act cumulatively in such a way that T_{\parallel} and T_{\perp} relax to a common value. The time for this relaxation (the second time scale) is exponentially long, or equivalently, the rate is exponentially small.

This paper presents a calculation of this exponentially small equipartition rate.² It also presents the results of molecular dynamics simulations that corroborate the existence of the adi-

*Supported by NSF grant PHY87-06358 and a grant of cpu time from the San Diego Supercomputer Center.

[†]Mathematical Institute, D.T.H., DK-2800 Lyngby, Denmark.

[‡]Dept. of Physics, Univ. of California, Berkeley, CA 94720.

abatic invariant and the value of the calculated rate,³ and it presents the results of recent experiments (with cryogenic pure electron plasmas) that are in agreement with the theory.⁴

In Section 2, we consider the isolated collision of two electrons in a strong magnetic field and calculate the exponentially small exchange of energy between the parallel and the perpendicular degrees of freedom. In Section 3, this energy exchange is used to calculate the equipartition rate for a plasma with $T_{\parallel} \neq T_{\perp}$. The analysis in this section employs a Boltzmann-like collision operator, which treats collisions as well separated binary interactions. The justification for this is that the most important collisions (most effective in producing energy exchange) are close collisions, and these tend to be well separated binary interactions—at least for a weakly correlated plasma. We consider only the case of weak correlation, and the experiments are carried out for this case.

The molecular dynamics simulations are presented in Section 4; the dynamics of 50 point charges that interact electrostatically in the presence of a uniform magnetic field is followed numerically for various values of the plasma parameters (density, temperature, and field strength). In Section 5, the results of the experiments are presented; a magnetically confined pure electron plasma is cooled to the cryogenic temperature range, and the equipartition rate is measured as a function of magnetic field strength and plasma temperature. For both the simulations and the experiments, the equipartition rate drops dramatically in accord with theory as the plasma enters the parameter regime of strong magnetization.

2. BINARY INTERACTION

In this section, we analyze an isolated collision between two electrons that interact electrostatically in the presence of a strong and uniform magnetic field, $\mathbf{B} = \hat{z}B$. The equations of motion for the electrons are

$$\frac{d\mathbf{v}_1}{dt} + \Omega\mathbf{v}_1 \times \hat{z} = \frac{e^2}{m} \frac{(\mathbf{r}_1 - \mathbf{r}_2)}{|\mathbf{r}_1 - \mathbf{r}_2|^3}, \quad (1)$$

$$\frac{d\mathbf{v}_2}{dt} + \Omega\mathbf{v}_2 \times \hat{z} = \frac{e^2}{m} \frac{(\mathbf{r}_2 - \mathbf{r}_1)}{|\mathbf{r}_1 - \mathbf{r}_2|^3}, \quad (2)$$

where \mathbf{r}_j and \mathbf{v}_j are the position and velocity of electron j . By adding and subtracting these equations, we obtain the two equations

$$\frac{d\mathbf{V}}{dt} + \Omega\mathbf{V} \times \hat{z} = 0, \quad (3)$$

$$\frac{d\mathbf{v}}{dt} + \Omega\mathbf{v} \times \hat{z} = \frac{e^2}{\mu} \frac{\mathbf{r}}{|\mathbf{r}|^3}, \quad (4)$$

where $\mathbf{V} = d/dt (\mathbf{r}_1 + \mathbf{r}_2)/2$ is the velocity of the center of mass, $\mathbf{r} = \mathbf{r}_2 - \mathbf{r}_1$ is the position of electron 2 relative to that of electron 1, $\mathbf{v} = d/dt (\mathbf{r})$ is the relative velocity, and $\mu = m/2$ is the reduced mass. The center of mass motion is equivalent to that of an electron in a uniform magnetic field, and the relative motion is equivalent to that of an electron in a uniform mag-

netic field and the field of a fixed charge. The solution for the center of mass motion is trivial, and the solution for the relative motion is simplified by the existence of an adiabatic invariant.

The condition for strong magnetization insures that the cyclotron frequency is much larger than any other frequency that characterizes the collisional dynamics [i.e., $\Omega \gg v_i/b$, v_i/b , where $|r| \geq b$]; so the cyclotron action $\mu v_i^2(t)/2\Omega$ is an adiabatic invariant. Since Ω is a constant, one can equivalently say that $\mu v_i^2(t)/2$ is an adiabatic invariant. Incidentally, the fact that $\mu v_i^2(t)/2$ is an invariant implies that the distance of closest approach is given by $b = e^2/(\mu v_i^2/2)$.

Note that $\mu v_i^2(t)/2\Omega$ is a new adiabatic invariant associated jointly with the two electrons; neither $m v_{i1}^2(t)/2\Omega$ nor $m v_{i2}^2(t)/2\Omega$ are valid invariants. For example, in Eq. (1), $r_2(t)$ is a time-dependent function that varies at the cyclotron frequency, and this breaks the adiabatic invariant of electron 1 [i.e., $m v_{i1}^2(t)/2\Omega \neq \text{const}$]. Likewise, the temporal variation of $r_1(t)$ breaks the adiabatic invariant of electron 2. By introducing the relative position and velocity (i.e., \mathbf{r} and \mathbf{v}), we have removed the explicit time dependence from the interaction and uncovered a new adiabatic invariant, $\mu v_i^2(t)/2\Omega$.

From Eq. (3), one can see that $V_i^2(t)$ is an exact constant of the motion; consequently, the relation $m v_{i1}^2(t)/2 + m v_{i2}^2(t)/2 = \mu v_i^2(t)/2 + (2m) V_i^2(t)/2$ implies that the sum of the perpendicular kinetic energies for the two electrons is an alternative expression for the adiabatic invariant. This expression can be generalized to the case where many electrons interact simultaneously, that is, the quantity $\sum_j m v_{j1}^2(t)/2$ is also an adiabatic invariant.^{1,2}

An adiabatic invariant is not strictly conserved but suffers exponentially small changes. For the case of a weakly correlated plasma, we will argue that the overall invariant [i.e., $\sum_j m v_{j1}^2(t)/2$] suffers changes primarily through close two-particle collisions; therefore we calculate the change that occurs in $\mu v_i^2(t)/2$ during a collision. From Eq. (4), it follows that

$$\frac{d}{dt} \frac{\mu v_i^2(t)}{2} = \frac{e^2 \mathbf{v}_i(t) \cdot \mathbf{r}_1(t)}{|\mathbf{r}(t)|^3} ; \quad (5)$$

thus, the quantity $\Delta(\mu v_i^2/2) = \mu v_i^2(\infty)/2 - \mu v_i^2(-\infty)/2$ is given by the time integral

$$\Delta \left[\frac{\mu v_i^2}{2} \right] = \int_{-\infty}^{+\infty} dt \frac{e^2 \mathbf{v}_i(t) \cdot \mathbf{r}_1(t)}{|\mathbf{r}(t)|^3} . \quad (6)$$

Following the usual practice in the theory of adiabatic invariants, we use the lowest-order orbits in evaluating the time integral, that is, we rewrite Eq. (6) as

$$\Delta \left[\frac{\mu v_i^2}{2} \right] \cong e^2 v_i \rho \int_{-\infty}^{+\infty} \frac{dt \cos(\Omega t + \delta)}{[\rho^2 + z^2(t)]^{3/2}} , \quad (7)$$

where (ρ, z) is the guiding center approximation for (r_1, z) , δ is a constant, and $z(t)$ is determined by

$$z^2 + \frac{2e^2/\mu}{[\rho^2 + z^2(t)]^{1/2}} = z^2(t = -\infty) = v_{if}^2 . \quad (8)$$

The origin of time may be shifted simply by changing the value of the constant δ ; so, without loss of generality, we choose the origin of time so that $z^2(t)$ is an even function of t , that is, so that the electron either passes $z=0$ or reflects at the time $t=0$. Equation (8) then reduces to the form

$$\Delta \left[\frac{\mu v_{\perp}^2}{2} \right] = e^2 v_{\perp} \rho \cos(\delta) \int_{-\infty}^{+\infty} \frac{dt \cos(\Omega t)}{[\rho^2 + z^2(t)]^{3/2}} . \quad (9)$$

In terms of the scaled variables

$$\zeta = z/b , \quad \xi = v_{\perp} t/b , \quad \eta = \rho/b , \quad \epsilon = v_{\perp}/\Omega b , \quad (10)$$

the time integral in Eq. (9) can be written as

$$\int_{-\infty}^{+\infty} \frac{dt \cos(\Omega t)}{[\rho^2 + z^2(t)]^{3/2}} = \frac{1}{v_{\perp} b^2} \int_{-\infty}^{+\infty} \frac{d\xi \cos(\xi/\epsilon)}{[\eta^2 + \zeta^2(\xi)]^{3/2}} , \quad (11)$$

and Eq. (8) can be rewritten as

$$\left[\frac{d\zeta}{d\xi} \right]^2 = 1 - \frac{1}{[\eta^2 + \zeta^2(\xi)]^{1/2}} . \quad (12)$$

Strong magnetization implies that $\epsilon \ll 1$, so the ξ integral in Eq. (11) involves the product of a rapidly oscillating function and a slowly varying function and turns out to be exponentially small. The integral can be evaluated by deforming the contour of integration into the complex ξ plane and is of the form²

$$\int_{-\infty}^{+\infty} \frac{d\xi \cos(\xi/\epsilon)}{[\eta^2 + \zeta^2(\xi)]^{3/2}} \equiv h(\epsilon, \eta) e^{-g(\eta)/\epsilon} , \quad (13)$$

where $h(\epsilon, \eta)$ is neither exponentially small nor exponentially large in the range of ϵ and η of interest, and $g(\eta)$ is given by

$$g(\eta) = \left| \int_1^{\eta} \frac{x^{3/2} dx}{\sqrt{(x-1)(\eta^2-x^2)}} \right| . \quad (14)$$

From the plot of $g(\eta)$ in Fig. 1, one can see that $g(\eta) \equiv \pi/2$ for $\eta = \rho/b \ll 1$ and that $g(\eta) \equiv \eta$ for $\eta = \rho/b \gg 1$. Thus, the ξ integral is of order $\exp[-\pi\Omega b/2v_{\perp}]$ for $\rho \ll b$ and of order $\exp[-\Omega\rho/v_{\perp}]$ for $\rho \gg b$. These exponentials are each of the form $\exp(-\Omega\tau)$, where τ characterizes the duration of the collision. Also, we note that the ξ integral is largest for collisions characterized by small impact parameter and large relative velocity.

3. CALCULATION OF THE EQUIPARTITION RATE

Next we turn to the question of how such collisions act cumulatively to produce the relaxation of T_{\parallel} and T_{\perp} in a strongly magnetized plasma. For simplicity, we consider the case of a

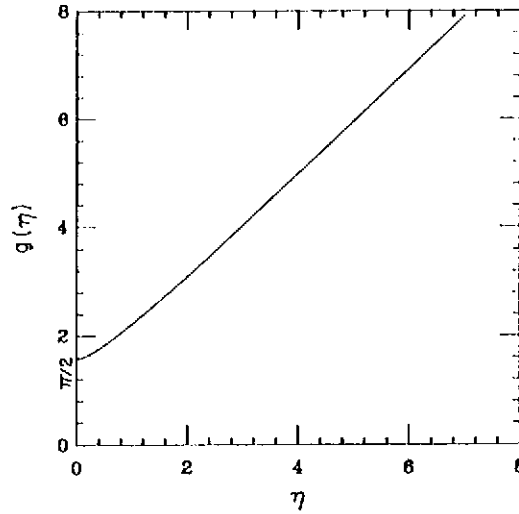


FIGURE 1

A plot of the function $g(\eta)$, defined in Eq. (14).

weakly correlated plasma, that is, a plasma in which $e^2 n^{1/3} \ll T_{\parallel}$, where n is the electron density. This inequality can be rewritten as the condition that $\bar{b} = e^2 / (\mu \bar{v}_{\parallel}^2 / 2) = 2e^2 / T_{\parallel}$ is small compared to the mean interparticle spacing (i.e., $\bar{b} \ll n^{-1/3}$). One can easily verify that correlations are determined by T_{\parallel} in the strongly magnetized parameter regime.

We have just seen that for the class of two-particle collisions it is the close collisions (i.e., $|\mathbf{r}_1 - \mathbf{r}_2| \cong \bar{b}$) that are most effective in producing an exchange of parallel and perpendicular energy. If we add a third particle into the dynamics, we obtain a small perturbation on the close two-particle collision unless all three particles are close simultaneously. We assume that the energy exchange caused by a close three-particle collision is of the same order as that for a close two-particle collision; this is reasonable considering time scale arguments concerning the durations of the collisions. Of course, the overall adiabatic invariant, $\sum_j m v_{j\parallel}^2(t)/2$, exists for

many-electron collisions. Since the inequality $\bar{b} \ll n^{-1/3}$ implies that close two-particle collisions are more frequent than close three-particle collisions, we neglect the close three-particle collisions and, similarly, all higher-order collisions. Also, we note that the close two-particle collisions are well-separated events (i.e., $|\mathbf{r}_1 - \mathbf{r}_2| \cong \bar{b} \ll n^{-1/3}$).

Such well-separated binary collisions can be treated with a Boltzmann-like collision operator.^{1,2,5} In particular, we evaluate the integral

$$\frac{dT_{\perp}}{dt} = \int d\mathbf{v}_1 \frac{m v_{1\perp}^2}{2} \frac{\partial f}{\partial t}(\mathbf{v}_1, t) \quad (15)$$

by replacing the time derivative of the distribution function with the Boltzmann-like operator

$$\frac{\partial f}{\partial t}(\mathbf{v}_1, t) = n \int 2\pi\rho d\rho \int d\mathbf{v}_2 |\hat{\mathbf{z}} \cdot (\mathbf{v}_2 - \mathbf{v}_1)| \times [f(\mathbf{v}'_1, t)f(\mathbf{v}'_2, t) - f(\mathbf{v}_1, t)f(\mathbf{v}_2, t)] . \quad (16)$$

In relation to the usual form of the Boltzmann collision operator, the integral over $2\pi\rho d\rho$ is equivalent to the integral over the impact parameter (or, scattering cross section), and the quantity $|\hat{\mathbf{z}} \cdot (\mathbf{v}_2 - \mathbf{v}_1)|$ replaces $|\mathbf{v}_2 - \mathbf{v}_1|$, since the two electrons stream toward one another along field lines. In the usual manner $(\mathbf{v}'_1, \mathbf{v}'_2)$ are velocities that evolve into $(\mathbf{v}_1, \mathbf{v}_2)$ during a scattering.

By substituting the collision operator into Eq. (15) and by using detailed balance, we obtain

$$\begin{aligned} \frac{dT_{\perp}}{dt} &= \frac{n}{4} \int 2\pi\rho d\rho \int d\mathbf{v}_1 \int d\mathbf{v}_2 |\hat{\mathbf{z}} \cdot (\mathbf{v}_2 - \mathbf{v}_1)| \\ &\quad \times [f(\mathbf{v}'_1, t)f(\mathbf{v}'_2, t) - f(\mathbf{v}_1, t)f(\mathbf{v}_2, t)] \\ &\quad \times \left[\frac{m v_{1\perp}^2}{2} + \frac{m v_{2\perp}^2}{2} - \frac{m v_{1\perp}^2}{2} - \frac{m v_{2\perp}^2}{2} \right] . \end{aligned} \quad (17)$$

The distribution functions are assumed to be of the form

$$f(\mathbf{v}_j, t) = \left[\frac{m}{2\pi T_{\perp}} \right]^{1/2} \left[\frac{m}{2\pi T_{\parallel}} \right] \exp \left[-\frac{m v_{j\perp}^2}{2T_{\perp}} - \frac{m v_{j\parallel}^2}{2T_{\parallel}} \right] . \quad (18)$$

To evaluate the multiple integral, it is convenient to introduce the center of mass velocity and the relative velocity (i.e., \mathbf{V} , and \mathbf{v}). With the aid of the relations

$$\begin{aligned} \frac{m v_{1\perp}^2}{2} + \frac{m v_{2\perp}^2}{2} &= \frac{\mu v_{\perp}^2}{2} + \frac{2m V_{\perp}^2}{2} , \\ \frac{m v_{1\parallel}^2}{2} + \frac{m v_{2\parallel}^2}{2} &= \frac{\mu v_{\parallel}^2}{2} + \frac{2m V_{\parallel}^2}{2} , \\ V_{\perp}^2 &= V_{\perp}^2 , \quad d\mathbf{v}_1 d\mathbf{v}_2 = d\mathbf{v} d\mathbf{V} . \end{aligned} \quad (19)$$

Eq. (17) can be rewritten as

$$\frac{dT_{\perp}}{dt} = \frac{n}{4} \int 2\pi\rho d\rho \int d\mathbf{v} |\mathbf{v}_{\perp}| [f_r(\mathbf{v}'_{\parallel}, \mathbf{v}'_{\perp}) - f_r(\mathbf{v}_{\parallel}, \mathbf{v}_{\perp})] \times \Delta(\mu v_{\perp}^2/2) , \quad (20)$$

where the integral over $d\mathbf{V}$ has been evaluated and

$$f_r(\mathbf{v}_{\parallel}, \mathbf{v}_{\perp}) = \left[\frac{\mu}{2\pi T_{\parallel}} \right]^{1/2} \left[\frac{\mu}{2\pi T_{\perp}} \right] \exp \left[-\frac{\mu v_{\parallel}^2}{2T_{\parallel}} - \frac{\mu v_{\perp}^2}{2T_{\perp}} \right] \quad (21)$$

is the distribution of relative velocities.

By using $\Delta(\mu v_{\perp}^2/2) = \mu v_{\perp}^2/2 - \mu v_{\perp}^2/2 = \mu v_{\perp}^2/2 - \mu v_{\perp}^2$, Eq. (20) can be rewritten as

$$\frac{dT_{\perp}}{dt} = \frac{n}{4} \int 2\pi\rho d\rho \int d\mathbf{v} |\mathbf{v}_{\perp}| f_r(\mathbf{v}_{\parallel}, \mathbf{v}_{\perp}) \Delta \left[\frac{\mu v_{\perp}^2}{2} \right] \times \left\{ \exp \left[\left[\frac{1}{T_{\parallel}} - \frac{1}{T_{\perp}} \right] \Delta \left[\frac{\mu v_{\perp}^2}{2} \right] \right] - 1 \right\} . \quad (22)$$

Taylor-expanding the exponential, substituting for $\Delta(\mu v_1^2/2)$ from Eq. (9), and integrating over $d v_1$ yields the expression

$$\frac{dT_1}{dt} = \left[T_1 \left[\frac{1}{T_1} - \frac{1}{T_{\parallel}} \right] \right] \frac{n}{4} \int 2\pi\rho d\rho \int d v_{\parallel} |v_{\parallel}| \times \frac{\exp(-\mu v_{\parallel}^2/2T_{\parallel})}{(2\pi T_{\parallel}/\mu)^{1/2}} \frac{e^4 \rho^2}{\mu} \left[\int_{-\infty}^{+\infty} \frac{dt \cos(\Omega t)}{[\rho^2 + z^2(t)]^{3/2}} \right]^2. \quad (23)$$

By using Eqs. (11) and (13) to reexpress the time integral, Eq. (23) reduces to the form

$$\frac{dT_1}{dt} = (T_{\parallel} - T_1) n \bar{b}^2 \bar{v}_{\parallel} I(\bar{\epsilon}),$$

$$I(\bar{\epsilon}) = \frac{\sqrt{2\pi}}{8} \int_0^{\infty} \frac{d\sigma}{\sigma} \exp\left[-\frac{\sigma^2}{2}\right] \times \int_0^{\infty} \eta^3 d\eta h^2 \left[\frac{1}{\bar{\epsilon}\sigma^3}, \eta \right] \exp\left[-\frac{2g(\eta)}{\sigma^3 \bar{\epsilon}}\right], \quad (24)$$

where we have introduced the scaled variables

$$\bar{v}_{\parallel} = \sqrt{T_{\parallel}/\mu}, \quad \sigma = v_{\parallel}/\bar{v}_{\parallel}, \quad \bar{b} = 2e^2/\mu\bar{v}_{\parallel}^2, \quad \bar{\epsilon} = \bar{v}_{\parallel}/\Omega\bar{b}. \quad (25)$$

Since $\bar{\epsilon}$ is assumed to be small and $g(\eta)$ is an increasing function of η , the main contribution to the η integral comes from small η . By making the approximations²

$$g(\eta) \cong g(0) + g''(0)\eta^2/2 = 1.57 + (0.675)\eta^2,$$

$$h(1/\bar{\epsilon}\sigma^3, \eta) \cong h(1/\bar{\epsilon}\sigma^3, 0) = 2.79(1/\bar{\epsilon}\sigma^3), \quad (26)$$

we obtain

$$I(\bar{\epsilon}) \cong (0.67) \int_0^{\infty} d\sigma \frac{e^{-\sigma^2/2}}{\sigma} e^{-(3.14)/(\bar{\epsilon}\sigma^3)}. \quad (27)$$

For small $\bar{\epsilon}$, the σ integral may be carried out by the saddle point method, and the result is

$$I(\bar{\epsilon}) = (0.47)\bar{\epsilon}^{1/5} e^{-(2.04)/\bar{\epsilon}^{2/5}}. \quad (28)$$

In Fig. 2, this small $\bar{\epsilon}$ asymptotic expression for $I(\bar{\epsilon})$ is compared to the results of a numerical evaluation of $I(\bar{\epsilon})$. The curve is a plot of the asymptotic expression, and the points are the result of numerical integration for various values of $\bar{\epsilon}$. One can see that the agreement is good for small enough values of $\bar{\epsilon}$.

The main point to note here is that the equilibration rate is larger than one might have guessed. Since the exchange of parallel and perpendicular energy for an isolated collision between two electrons is exponentially small in $1/\bar{\epsilon}$, one might have guessed that the equilibration rate would be exponentially small in $1/\bar{\epsilon}$. However, the equilibration rate turns out to be exponentially small in $1/\bar{\epsilon}^{2/5}$, and this distinction is important since $\bar{\epsilon}^{-2/5} \gg \bar{\epsilon}$ for $\bar{\epsilon} \ll 1$.

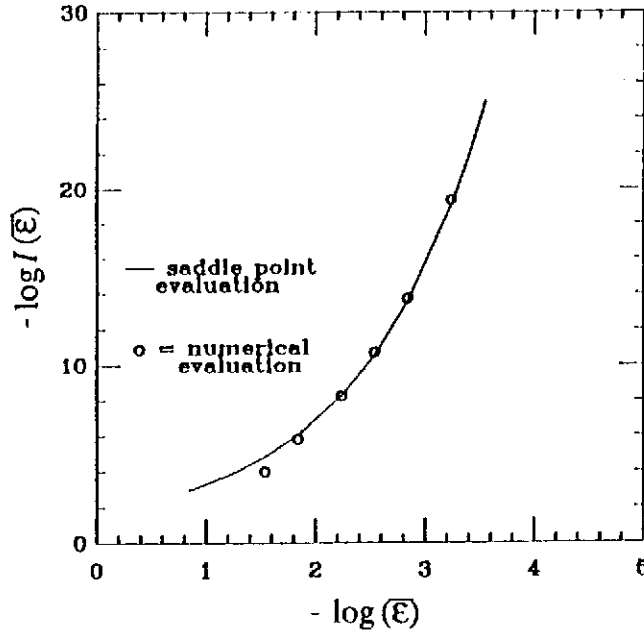


FIGURE 2

The saddle point evaluation of $I(\bar{\mathcal{E}})$ compared to the result of a numerical evaluation of $I(\bar{\mathcal{E}})$ for various values of $\bar{\mathcal{E}}$.

The $1/\bar{\mathcal{E}}^{2/5}$ dependence is determined by a competition between the velocity dependence of $\exp(-2\pi/\mathcal{E}) = \exp(-4\pi e^2 \Omega / m v_{\parallel}^3)$ and the velocity dependence of the distribution of relative velocities, $\exp(-\mu v_{\parallel}^2 / 2T_{\parallel})$. Collisions characterized by large relative velocity are particularly effective at producing an exchange of parallel and perpendicular energy, but there are relatively few such collisions.

4. MOLECULAR DYNAMICS SIMULATION

This section presents the results of molecular dynamics simulations.³ The dynamics for $N = 50$ point charges that interact electrostatically and move in a uniform magnetic field is followed numerically, and the equipartition rate is determined for various values of the plasma parameters (density, temperature, and field strength).

For computational convenience, it is useful to scale velocities by $\bar{v}_{\parallel} = \sqrt{T_{\parallel}/\mu}$, distances by $\bar{b} = 2e^2/\mu\bar{v}_{\parallel}^2$, and times by $\bar{b}/\bar{v}_{\parallel}$. With these units, the equations of motion take the form

$$\dot{\mathbf{x}}'_i = \mathbf{v}'_i, \quad \dot{\mathbf{v}}'_i = \frac{1}{\bar{\mathcal{E}}} \mathbf{v}'_i \times \hat{z} + \frac{1}{4} \sum_{i \neq j}^N \frac{\mathbf{x}'_i - \mathbf{x}'_j}{|\mathbf{x}'_i - \mathbf{x}'_j|^3}, \quad i = 1, \dots, N, \quad (29)$$

where primes signify scaled variables. Because we need to evaluate the full Coulomb force term, the number of floating point operations associated with each reference to this set of equations scales roughly quadratically with the number N of particles in the system; this is the main

obstacle to a simulation involving a realistically large number of particles. Nevertheless, a glimpse of the phenomena has been obtained with a simulation involving 50 interacting particles, performed on the SDSC CRAY X-MP.

As initial conditions, we take the 50 particles to be uniformly distributed spatially inside a box $-L/2 < (x, y, z) < +L/2$, of volume L^3 , and with initial velocities picked from a bi-Maxwellian velocity distribution with $(T_{\perp}/T_{\parallel})=0.2$. As the system evolves, the particles are confined in the z direction by specular reflections at the walls at $z = \pm L/2$. Confinement in the radial direction is ensured, since the total canonical angular momentum P_{θ} is a constant of the motion and provides a constraint on the allowed radial positions of the electrons.⁶ Another constant of the motion is the total energy; we employ a high precision Bulirsch-Stoer ODE solver⁷ and find during a typical run that the total energy is conserved to order $\Delta E/E \sim 10^{-7}$ and that the total canonical angular momentum is conserved to order $\Delta P_{\theta}/P_{\theta} \sim 10^{-5}$.

From a statistical (or macroscopic) perspective, the scaled system is characterized by two parameters: $\bar{\epsilon}$ and L' . Here, we have in mind fixed $N = 50$, fixed initial $T_{\perp}/T_{\parallel} = 0.2$, and fixed initial $\langle v_{\parallel}^2 \rangle = (T_{\perp}/m)/(T_{\parallel}/\mu) = 1/2$. The parameter $\bar{\epsilon}$ is a measure of the magnetic field strength, and the parameter L' is a measure of density $n' = N/L^3$. By decreasing L' , we increase the collision frequency (ν_{ee}), or equivalently, we increase the correlation strength ($\Gamma = e^2/aT_{\parallel}$, where $4\pi n a^3/3 = 1$). Not all of the $(\bar{\epsilon}, \Gamma)$ parameter plane is physically accessible. For a nonneutral electron plasma, the Brillouin limit⁸ (i.e., $\omega_p < \Omega/\sqrt{2}$) specifies the maximum density that can be confined for a given magnetic field strength, and in terms of $\bar{\epsilon}$ and Γ this limit takes the form $\bar{\epsilon}\Gamma^{3/2} < 1/\sqrt{12}$.

Some sample results are shown in Figs. 3(a) and 3(b), where W_{\perp}/W and W_{\parallel}/W are plotted as functions of time. Here, W_{\perp} and W_{\parallel} refer to the total perpendicular and parallel kinetic energies, respectively, and $W = W_{\perp} + W_{\parallel}$. The dashed lines mark the values predicted by the equipartition theorem: $W_{\perp}/W = 2/3$ and $W_{\parallel}/W = 1/3$. Figure 3(a) shows the results of a run with low magnetic field strength ($\bar{\epsilon} = 14$) and Fig. 3(b) shows the results of a run with large field strength ($\bar{\epsilon} = 0.14$) but the same correlation strength (i.e., $\Gamma = 0.03$). One can see that the increased field suppresses the relaxation. To investigate the rate equation numerically [i.e., Eq. (28)], we examined the initial rate of temperature equilibrium for a bi-Maxwellian velocity distribution with $T_{\perp} = 0.2T_{\parallel}$. In order to suppress statistical fluctuations without going to a large number of particles, we averaged the change in perpendicular and parallel kinetic energy over 20 different sets of initial conditions. These were advanced forward a time Δt short compared with the equipartition time, but long enough for a least-squares fit to the slope of the evolving $W_{\perp}(t) = NT_{\perp}(t)$. In Fig. 4, the analytic prediction $(dT_{\perp}/dt)[(T_{\parallel} - T_{\perp})n\bar{b}^2v_{\parallel}]^{-1} = I(\bar{\epsilon})$ is compared to numerical values of $(\Delta T_{\perp}/\Delta t)[(T_{\parallel} - T_{\perp})n\bar{b}^2v_{\parallel}]^{-1}$ for various values of $\bar{\epsilon}$ and Γ . One can see that the numerical values are insensitive to the value of Γ and follow the $I(\bar{\epsilon})$ curve quite well, although the agreement is best in the small $\bar{\epsilon}$ limit. This is to be expected, since $I(\bar{\epsilon})$ was obtained in the small $\bar{\epsilon}$ asymptotic limit.

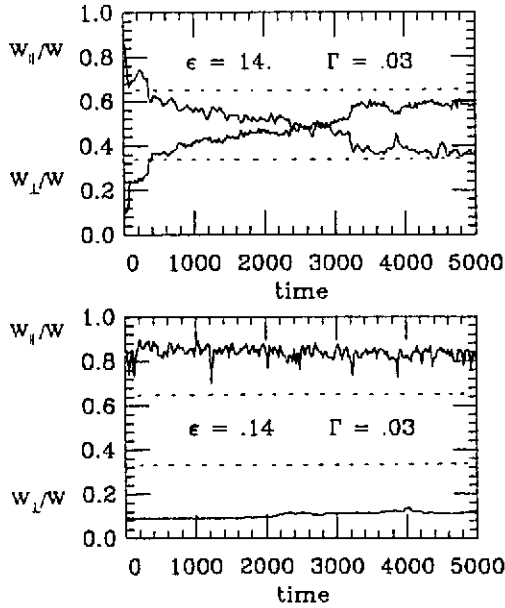


FIGURE 3
Evolution of W_{\perp}/W and W_{\parallel}/W (a) for weak magnetic field (i.e., $\bar{\epsilon}=14$) and (b) for strong magnetic field (i.e., $\bar{\epsilon}=0.14$).

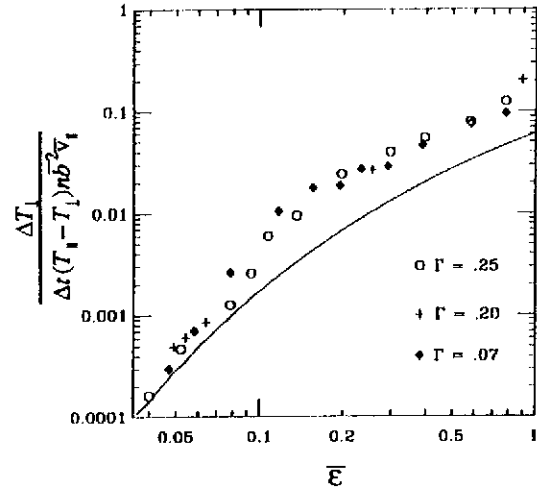


FIGURE 4
Comparison of the function $I(\bar{\epsilon})$ (solid curve) to values of $(\Delta T_{\perp}/\Delta t)[(T_{\perp}-T_{\parallel})nb^{-2}v_{\perp}^{-1}]^{-1}$ obtained from the simulations.

V. EXPERIMENT

The condition for strong magnetization can be written as $\Omega \gg \bar{v}/b$, or equivalently, as $T^{3/2}(\text{eV}) \ll 10^{-7}B(\text{G})$, where for simplicity we have set $T_{\perp}=T_{\parallel}=T$. One can see that strong magnetization requires low temperature as well as large magnetic field; even for B as large as 100 kG, the required temperature [$T \ll (.05)\text{eV}$] is such that a neutral plasma would recombine. However, a pure electron plasma cannot recombine, since there are negligibly few ions in the confinement region. Recent experiments have succeeded in cooling a magnetically confined pure electron plasma to the cryogenic temperature range (where the plasma is strongly magnetized) and in measuring the equipartition rate as a function of plasma temperature and magnetic field strength.⁴

A schematic diagram of the confinement apparatus used in these experiments is shown in Fig. 5. A conducting cylinder is divided into several electrically isolated sections (only three of which are shown), and the whole apparatus is immersed in a magnetic field that is nearly axial and uniform in the region of the plasma. The plasma resides in the central grounded cylinder, with radial confinement provided by the axial magnetic field and axial confinement provided by electrostatic fields. The two end cylinders are biased sufficiently negative to provide this axial

confinement. The plasma density for these experiments is of order 10^9 cm^{-3} and the initial plasma temperature is of order 10 eV . The magnetic field is provided by a superconducting coil, and field strengths up to 60 kG are used.

Immediately after the plasma is trapped, it begins to cool by cyclotron radiation, and the radiated energy is absorbed by the walls, which are maintained at 4°K . Each electron radiates according to the Larmor formula⁹ (the plasma is optically thin), and this leads to an exponential decrease in plasma temperature with a time constant $\tau = 4 \times 10^8 / B^2 \text{ sec}$, where B is in Gauss. For example, for $B = 60 \text{ kG}$, the time constant is .1 sec. This time is long compared to the equipartition time over the whole parameter range explored in the experiments, so T_{\parallel} remains nearly equal to T_{\perp} even though cyclotron radiation extracts only perpendicular kinetic energy.

The temperature T_{\parallel} is measured by letting the plasma gradually escape to the collector [see Fig. 5]. As the potential on the cylindrical section in front of the collector is gradually increased (toward zero), electrons in the tail of the Maxwellian velocity distribution begin to make it over the potential barrier and reach the collector. The temperature is determined by measuring the current collected as a function of the potential and fitting to a Maxwellian. Of course, dumping the plasma in this manner is a destructive procedure, and the experiments rely on shot to shot reproducibility. By measuring the temperature as a function of time after injection, one can follow the radiative cooling of the plasma, and the measured temperature tracks the theoretical expectation down to about 50°K , which is very likely the present limit of the temperature diagnostic.

To determine the equipartition rate, a small oscillating component is added to the potential on one of the end cylinders. This acts like an electrostatic piston that alternately compresses and expands the plasma in the axial direction. If the oscillation frequency is low compared to the equipartition rate, the compression and expansion cycle is a reversible process (a 3-D compression and expansion characterized by $c_p/c_v = (f + 2)/f = 5/3$). Likewise, if the oscillation frequency is large compared to the equipartition rate, the cycle is a reversible process (a 1-D adiabatic compression and expansion characterized by $c_p/c_v = (f + 2)/f = 3$). However, when the oscillation frequency is comparable to the equipartition rate, the process is not reversible. More work is done during the compression stroke than is given back during the expansion stroke, and the excess appears as plasma heat. One can easily show that the heat per cycle is a maximum for $\omega = 3\nu$, where ω is the angular frequency of the oscillation and ν is the equipartition rate [i.e., $dT_{\perp}/dt = \nu(T_{\parallel} - T_{\perp})$]. To understand the factor of 3, note that in the absence of heating the definition of ν implies that $d(T_{\perp} - T_{\parallel})/dt = 3\nu(T_{\parallel} - T_{\perp})$.

In the experiments, the oscillation frequency is adjusted so that the heating per cycle is maximum. Also, the oscillation amplitude is adjusted so that the heating just balances the cooling due to radiation, and the plasma temperature remains constant. This procedure is then repeated for various values of the temperature and magnetic field strength, and the equipartition rate is measured as a function of these parameters. In Fig. 6, the points are measured values and the curves are theoretical predictions. The dashed curve applies to a weakly magnetized

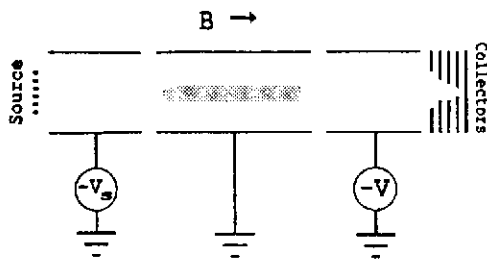


FIGURE 5

Schematic diagram of the confinement apparatus.

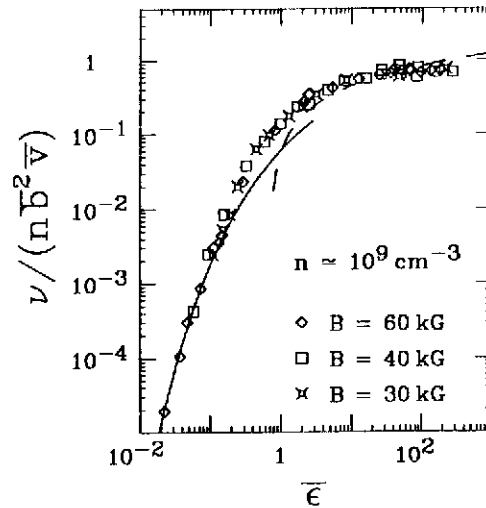


FIGURE 6

Comparison of measured equipartition rate to theory.

plasma ($\bar{\mathcal{E}} > 1$); it is the prediction of Ichimaru and Rosenbluth¹⁰ as modified by Montgomery, Joyce and Turner's¹¹ prescription for the Coulomb logarithm [i.e., $\ln(\lambda_D/b) \rightarrow \ln(\bar{\mathcal{E}})$]. For strong magnetization ($\bar{\mathcal{E}} < 1$), the solid curve is the function $I(\bar{\mathcal{E}})$ given in Eq. (28). One can see that the measured rate drops dramatically for $\bar{\mathcal{E}} \ll 1$ in good agreement with theory.

REFERENCES

- 1) T.M. O'Neil, *Phys. Fluids* **26** (1983) 2128.
- 2) T.M. O'Neil and P.G. Hjorth, *Phys. Fluids* **28** (1985) 3241.
- 3) P.G. Hjorth and T.M. O'Neil, *Phys. Fluids* **30** (1987) 2613.
- 4) B. Beck, J. Fajans, and J.H. Malmberg, *Bull. Am. Phys. Soc.* **33** (1988) 2004.
- 5) G. Uhlenbeck and G. Ford, *Lectures in Statistical Mechanics* (AMS, Providence, Rhode Island, 1963) 118.
- 6) T.M. O'Neil, *Phys. Fluids* **23** (1980) 2216.
- 7) W.H. Press, B.P. Flannery, S.A. Teukolsky, and W.T. Vetterling, *Numerical Recipes* (Cambridge University Press, London, England, 1966).
- 8) R.C. Davidson, *Theory of Nonneutral Plasmas* (Benjamin, Reading, Massachusetts, 1974) 4.
- 9) J.D. Jackson, *Classical Electrodynamics* (Wiley, New York, 1975) 659.
- 10) S. Ichimaru and M.N. Rosenbluth, *Phys. Fluids* **13** (1970) 2778.
- 11) D. Montgomery, G. Joyce, and L. Turner, *Phys. Fluids* **17** (1974) 2201.